Instrumentation and Measurement
Technology Conference – IMTC 2007
Warsaw, Poland, May 1-3, 2007

A Far-Range Off-line Camera Calibration Method for Stereo Lane Detection Systems

András Bódis-Szomorú and Tamás Dabóczi

Budapest University of Technology and Economics
Dept. of Measurement and Information Systems
H-1117 Budapest, Magyar tudósok krt. 2., HUNGARY
Phone: +36 1 463-2065, Fax: +36 1 463-4112
Email: bodis@mit.bme.hu, daboczi@mit.bme.hu

Zoltán Fazekas

Systems and Control Laboratory
Computer and Automation Research Institute
H-1111 Budapest, Kende u. 13-17., HUNGARY
Phone: +36 1 279 6173
Email: zfazekas@sztaki.hu

Abstract – A far-range camera calibration method for vision sensors used in automatic lane detection systems is investigated. Autonomous vehicle guidance based on stereo image acquisition requires the knowledge of the camera parameters, such as camera position, orientation, lens distortion, focal length etc. with high precision. Calibration is performed by placing markers in known positions in front of the vehicle holding the camera(s) and by detecting the location of their images in the acquired snapshots. The parameters are then estimated by minimizing the geometric error in the image. Most of the methods discovered in the literature do not consider errors in the measurement of marker locations. However, a precise marker arrangement for far-range calibration might be expensive to set up. This paper shows that imprecision in the 3D location of the markers can not be tolerated in some practical situations and in such cases, a different optimization is proposed in the calibration of the extrinsic camera parameters (camera position and orientation). A position estimation method is also shown to extract marker positions from far-range laser distance meter measurements. The estimated marker positions are corrected by considering aiming errors, as well. Parameter errors are also estimated. It will be shown that our new calibration and optimization method is expected to result a good accuracy compared to commercial methods.

Keywords – camera calibration, lane detection, stereo vision, autonomous vehicle guidance.

I. INTRODUCTION

Automatic lane detection plays an important role in the autonomous lateral control of on-road vehicles. The objective of such systems is to increase safety by determining the exact position of the vehicle within the actual lane, detecting lane curvature, predicting vehicle trajectory and actuating through the electronic braking system (EBS) or through the electronic power assisted steering system (EPAS). For this purpose, the application of vision sensors in autonomous lane following is usually preferred to laser sensors and radar, as vision sensors are of non-intrusive nature and they do not require additional infrastructure. Stereo systems [1] are capable of achieving higher accuracy in 3D lane geometry reconstruction than mono systems relying on simplifying assumptions do. However, the fulfillment of this potential heavily depends on the quality of camera calibration.

Stereo systems reconstruct road geometry by first detecting feature points of the current lane within a predicted region of interest in the two images separately [1]. Then data from the two sources is fused by searching for point correspondences using correlation techniques (stereo matching) [2]. The pair of a selected feature point in one of the images lies on a specific line (epipolar line) in the other image [2,3]. This constraint extremely simplifies the search and is resulted from the rigid stereo geometry of the cameras that are fixed to the vehicle chassis. The matching points are reprojected in space with triangulation [3] and a lane model is fitted to the resulted point cloud [1]. If camera parameters are inaccurate, the computed epipolar line is shifted and stereo matching might fail [4], on the one hand, and the triangulation might result intolerable inaccuracies in the reprojected point coordinates, on the other hand. Therefore, a precise preliminary far-range camera calibration is indispensable for these systems.

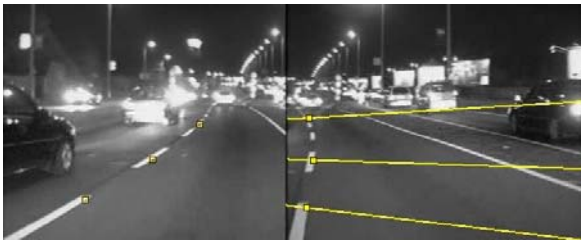

Fig. 1. Stereo matching: the correspondent of the highlighted points in the left image is searched along epipolar lines in the right image.

The most common approach for camera calibration is to make snapshots of a checkerboard pattern in different orientations and then to estimate the camera parameters by minimizing geometric error in the image [5,6]. This relies on the assumption that the marker arrangement (checkerboard pattern) is printed accurately and is

planar [5]. In far-range calibration this is not the case since a precise marker arrangement is expensive to set up. For such cases, we propose a method for measuring the marker locations in space with laser distance meters. Then we propose a two-step calibration method: first the intrinsic parameters (relative focal lengths, principal point, distortion coefficients, skew) and then the extrinsic parameters (camera location and orientation in the world reference frame) are calibrated. A modification of a commonly used optimization method for the extrinsic parameter estimation is proposed that takes into consideration inaccuracies in 3D marker locations, as well. A convenient confidence computation of the estimated camera parameters is also presented. Finally, we evaluate the new method with simulations and show some experimental results.

II. OVERVIEW OF THE CALIBRATION PROCESS

Intrinsic parameters are determined independently for the two cameras with the checkerboard-method proposed by Z. Zhang [5] because of its simplicity and high accuracy considering the internal parameters. The checkerboard covers the full field-of-view of the camera and can provide lens-distortion information in all the regions of the image. The *extrinsic parameters* (camera location and orientation) are then calibrated for far-range with a different method.

The proposed calibration process consists of the following steps:

(1) Calibrating the *intrinsic camera parameters* of the two cameras independently with the checkerboard-method. For later use, let us denote the vector of intrinsic camera parameters by $\mathbf{p_{int}}$.

(2) Driving the vehicle that holds the two cameras to an open flat area of about 15 meters wide and 40 meters long.

(3) Placing marker plates of 50x50 cm with an X-like figure in a predefined arrangement in front of the vehicle within the common field of view of the two cameras up to 30-35 meters (Fig. 2. shows the perspective view of such an arrangement). The precise placement is not relevant.

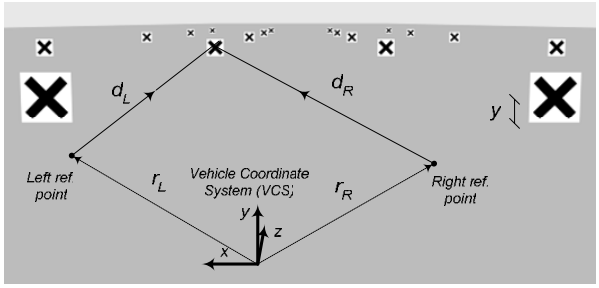

Fig. 2. Perspective view of the marker arrangement for extrinsic calibration and the two-point distance measurement arrangement.

(4) Designating two reference points ($\mathbf{r_L}$ and $\mathbf{r_R}$ vectors) on the left and on the right side of the vehicle on the ground. The position of the reference points has to be exactly measured in the vehicle's reference frame that is fixed to the vehicle chassis but its origin can be designated freely e.g. on the ground. After the calibration measurements this reference frame should be translated to the vehicle's center-of-gravity.

(5) Placing laser distance meters above the designated reference points and aiming at each table one-by-one. Measuring the distance of the markers from the two reference points.

(6) Taking a close-range photo of the markers with a digital camera when the marker is aimed at with the distance meter. The laser dot must be visible on the marker. Measuring the aiming errors by automatically evaluating the photos. This is required for measurement correction.

(7) From the distances, calculating the 3D coordinates of the marker centers $\mathbf{x_i}=(x_i,y_i,z_i)^T$ in the measurement reference system (located between the reference points, see Fig. 2.) which is in known position in the vehicle coordinate system. The result of step 6 is used here.

(8) Make a snapshot of the calibration scene with the two cameras independently and determine the $\mathbf{x_i'}=(x_i',y_i')^T$ coordinates of all the marker centers in the snapshots.

(9) Run the optimization proposed in this paper to estimate *extrinsic camera parameters* (for later use, let us denote the vector of extrinsic camera parameters by $\mathbf{p_{ext}}$) and determine the estimation errors for all intrinsic and extrinsic parameters.

III. DETERMINING MARKER COORDINATES IN SPACE AND IN THE IMAGES

The objective of steps 2-7 is to determine the coordinates of the marker centers in the measurement reference frame (Fig. 2.). The location of the markers (depth and lateral position) is measured from two reference points with laser distance meters by aiming at each of the markers. This presumes a totally flat field: the height of the marker centers is assumed to be constant. When this is not the case it seems to be convenient to perform distance measurements from three reference points and then estimate all the three coordinates of the marker centers. However, this is not suggested because the estimation of the center of marker heights becomes ill-posed. Based on geometrical considerations, the marker position $\mathbf{x}(\mathbf{p_m})=[x(\mathbf{p_m}),y(\mathbf{p_m}),z(\mathbf{p_m})]^T$ can be estimated from the preferred two-point measurement. Corresponding to Fig. 2., the parameter vector $\mathbf{p_m}$ can be written as:

$$p_m = (y_M, d_L, d_R, r_L^T, r_R^T, \delta_A^T, \delta_B^T, \alpha^T)^T. \qquad (1)$$

d_L and d_R are the measured distances and $\boldsymbol{\delta_L}=(\delta_{Lx},\delta_{Ly})^T$, $\boldsymbol{\delta_B}=(\delta_{Rx},\delta_{Ry})^T$ are the aiming errors at each marker. The vector $\boldsymbol{\alpha}$ contains the yaw, pitch and roll

angles of the marker plate, if the marker plate is not parallel to the xy plane due to an imprecise placement.

This geometrical arragement is described by the following two equations:

$$d_R^2 = \left\| x + Q(\alpha)\delta_R - r_R \right\|_2^2 \qquad (2)$$
$$d_L^2 = \left\| x + Q(\alpha)\delta_L - r_L \right\|_2^2,$$

where $\mathbf{Q(\alpha)}$ is a 3x2 matrix describing the rotation between the VCS and the marker plate. These equations are directly applicable in the simulation of the measurements. However, the marker center's position $\mathbf{x}$ is to be determined in a practical situation. In such a case, the equation can be easily solved numerically e.g. using *fsolve* in MATLAB. A good initial guess can be found by neglecting $\mathbf{Q}$ because $\mathbf{Q}$ models only small inaccuracies in the marker placement.

δ_L and δ_R can be measured by taking a close-range snapshot (with a digital camera) from each marker when it is aimed with the laser beams (Fig. 3., left image). From these snapshots, with the assumption that the exact sizes of the marker plates are known, $\boldsymbol{\delta_L}$ and $\boldsymbol{\delta_R}$ errors can be automatically measured with the metrical rectification [3] of the markers in the snapshots. This requires the detection of the four corners of the plate. The precision of $\boldsymbol{\delta_L}$ and $\boldsymbol{\delta_R}$ depends on the resolution of the snapshot and is typically in the millimeter range. This assumes that the tripod of the laser distance meter is stable and the laser dot does not move significantly at the moment of the measurement.

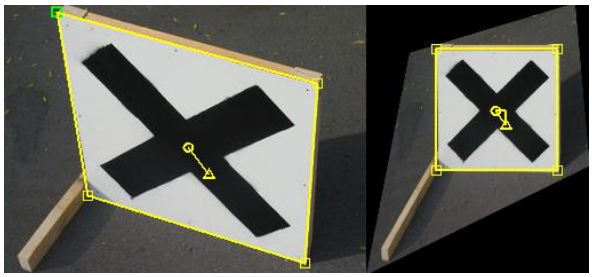

Fig. 3. Automated aiming error detection on the snapshots created with a digital camera: original image and metrically rectified image (o: center of gravity, Δ: detected location of the laser dot).

The precision of the marker position estimation can be computed by linearizing equations (2), by expressing the infinitesimal error vector $\boldsymbol{\Delta x}$ in function of all the other parameters and by evaluating the analytically available Jacobian $\mathbf{J_m}$ of $\mathbf{x}(\mathbf{p_m})$ at the measured parameter vector $\mathbf{p_{est}}$. The distribution of each measurement is modeled as Gaussian. In practice, the worst-case deviation of each parameter can be estimated, and e.g. the 99% confidence level may be set based on these estimations. This is required for the mathematical tractability of the estimation problem and must not fall too far from the reality. Then the diagonal covariance matrix $\boldsymbol{\Sigma_m}$ of the independent measured parameters can be built up and the covariance of the marker location estimation can be computed by forward-propagating the uncertainties through the linearized model:

$$\Sigma = J_m \Sigma_m J_m^T , \qquad (3)$$

$\boldsymbol{\Sigma}$ or the derived worst-case (or 99%) estimation error $\boldsymbol{\Delta x_i}$ characterizes the inaccuracy of the location estimation $\mathbf{x_i}$ for the i-th marker and this experimental information can be used in the optimization step.

The next step (step 8) is to detect the X-shaped markers (Fig. 2*.) in the image* acquired by the two cameras as well and to compute the center of gravity of each marker in both images. Center of gravity computation relies on many pixels forming the image of the markers and therefore this is a regression-like problem. On the one hand, this results sub-pixel precision in a robust manner, on the other hand this implies that the supposition of a 2D isotropic Gaussian noise present in the marker center coordinates is again not very far from the reality (due to the symmetries in the marker shape and due to the central limit theorem).

The markers are detected in the images automatically by using an FFT-based fast normalized cross correlation method with an X-template. After that the black X's are located, the center of gravity of the thresholded and inverted subimage is computed. The thresholding serves for robustness (for the case when the pattern is shaded).

The error of the X-detector can be estimated by applying it to synthetic images. A tiled pattern is generated with randomly rotated and appropriately resized X-templates. These templates are rasterized at precisely known positions. The small random rotations model the effect of the marker placement uncertainties. A Gaussian filter is applied on the tiled pattern and additive noise is superimposed, as well. Since the exact location of the markers is known, a detection error analysis can be easily performed.

Let us denote with $\mathbf{x_i'}=(x_i',y_i')^T$ and $\boldsymbol{\Sigma_i'}$ the center coordinates of the i-th marker detected in the image and the estimated covariance related to it, respectively.

IV. ESTIMATION OF THE CAMERA PARAMETERS

Step 1 and step 9 (in section II.) together form a two-step calibration algorithm. A general camera model used in the optimizations can be formulated as:

$$x' = \varphi(p, x) , \qquad (4)$$

where the nonlinear mapping φ parameterized with the parameter vector $\mathbf{p=(p_{int}^T, p_{ext}^T)^T}$ of all the intrinsic and extrinsic parameters maps any 3D-point $\mathbf{x}$ into a 2D-point $\mathbf{x'}$. $\mathbf{x}$ is given in metrical coordinates and $\mathbf{x'}$ is given in pixel coordinates. In the most common cases the camera model for a single camera is the pinhole model extended with a distortion model (typically radial and tangential distortion model) [2,3,6]. The camera model we use is that used in [2] extended with a 4th order radial distortion model [5]:

$$X_c = R(X - t) \tag{5}$$

$$X_p = \left(\frac{x_c}{z_c}, \frac{y_c}{z_c}\right)^T = (x_p, y_p) \tag{6}$$

$$X_d = (1 + d_1 r^2 + d_2 r^4)\begin{bmatrix} x_p - c_x \\ y_p - c_y \end{bmatrix} + \begin{bmatrix} c_x \\ c_y \end{bmatrix} \tag{7}$$

$$X' = \begin{bmatrix} -f_x & s \\ 0 & -f_y \end{bmatrix} X_d + \begin{bmatrix} u_0 \\ v_0 \end{bmatrix} \tag{8}$$

Here in (5) R is the 3x3 camera rotation matrix with 3 degrees of freedom, **t** is the camera translation vector. (7) is the radial distortion model: c_x, c_y are the (metrical) coordinates of the radial distortion center, d_1, d_2 are the radial distortion coefficients. Such a distortion model is satisfying in most of the cases. Radial distortion is modeled before rasterization (8) because the distortion is elliptical in pixel coordinates. f_x, f_y are the relative focal lengths in pixel coordinates, s is the axis skewness parameter, u_0 and v_0 are the principal point coordinates. The vector of the intrinsic and extrinsic parameters can be written as:

$$p_{int} = (f_x, f_y, s, u_0, v_0, c_x, c_y, d_1, d_2)^T, \tag{8}$$

$$p_{ext} = p_{ext}(r^T, t^T)^T, \tag{9}$$

where **r** is the rotation vector related to **R** by the Rodrigues-formula. Thus, we have 9 intrinsic and 6 extrinsic camera parameters, as a first approach.

Step 1 results an estimate for the vector of intrinsic parameters $\mathbf{p_{int}}$ from the known metrical coordinates of the square–corners in the checkerboard pattern and from the measured pixel-coordinates of the same corners in the snapshots taken of the pattern in different orientations. It should be noted that each additional checkerboard snapshot requires a new $\mathbf{p_{ext,i}}$ vector that describes the relative orientation and location of the camera and the checkerboard.

The parameters are determined by iteratively minimizing the sum of the geometric errors $\|\boldsymbol{\varepsilon}_{ij}\|^2$ for all the square points *j=1,2...n* in all the images *i=1,2...m* [5,6]. The optimal estimate $\mathbf{p_{opt}}$, is proved to be maximum likelihood (ML) [3,5]. The checkerboard method is well applicable in far-range calibration as well, but only for the estimation of the intrinsic parameters. The many external parameters (checkerboard positions and orientations) resulted are not relevant for us here.

After finding the optimal estimate, the residual errors can be computed for each feature point. This is very close to a uniform, isotropic Gaussian distribution which implies that the precision of the intrinsic parameter estimation is well represented by a single deviation parameter computed from the residual errors. The uncertainty is then backward propagated to camera parameters (very similarly to (3)). This requires the knowledge of the Jacobian of the camera model φ evaluated at $\mathbf{p_{opt}}$. Therefore, the outputs of step 1 are the intrinsic parameters ($\mathbf{p_{int}}$) and the covariance matrix $\boldsymbol{\Sigma}_{\mathbf{int}}$ related to them.

Step 9 results an estimate for the vector of extrinsic parameters $\mathbf{p_{ext}}$ from the known 3D metric coordinates ($\mathbf{x_i}$) of the X-shaped markers and from the measured 2D pixel-coordinates ($\mathbf{x_i'}$) of the marker centers extracted from the two images taken of the calibration scene with the stereo vision system. The extrinsic camera parameters are determined independently for the two cameras and then the extrinsic parameters of the stereo rig can be computed at any time from the result of the independent calibrations [2]. This method is used because not only the relative location and orientation of the cameras is relevant but the absolute position and orientation of the stereo rig in the vehicle's reference system, as well [4].

Here, a usual choice is to minimize the geometric error in the image only:

$$C(p) = \sum_{i=1}^{n} \left\| x_i' - \varphi(p, x_i) \right\|^2, \tag{10}$$

where n is number of feature points (X-markers) used in the calibration. This means that the inaccuracies in the (3D) metrical marker coordinates are all translated into a geometric error in the image and also that it might be irrelevant to suppose an isotropic Gaussian distribution that is uniform in the whole image, especially when calibrating for far range and the depth range is wide. However, if nothing is known about the noise structure, this is the best we can do.

In [4], an alternative method is presented, however they apply nonlinear equation solving and therefore they minimize an algebraic error that is not related to physical quantities. In the meantime, they do not deal with radial distortion models that can cause significant error in lane reconstruction.

We propose a different solution which exploits all the experimental information we can have about the noise structure, which minimizes geometrical errors and which can deal with radial distortion models due to its generality. Using the proposed method we minimize errors in the 3D metrical space and in the images simultaneously and we sum the terms by weighting them with the inverse of their confidence level. The

Therefore we suggest building in the inaccuracy information $\boldsymbol{\Sigma}_i$ and $\boldsymbol{\Sigma}_i'$ resulted from our preliminary experimental considerations into the cost function. If the noise distribution is Gaussian, this approach leads to the general maximum likelihood solution that can be found in [2] as a theoretical possibility but its application is rarely found in the camera calibration practice:

$$C(p_{ext}, q_i) = \sum_{i=1}^{n} \left\{ \left\| x_i' - \varphi(p, x_i) \right\|_{\Sigma'}^2 + \left\| x_i - q_i \right\|_{\Sigma}^2 \right\} \quad (11)$$

We need to recall this general ML cost function mainly due to the relatively high (and known) inaccuracies in the 3D measurements. It can be seen that additional terms are present in the general solution right next to the widely used terms. The Mahalanobis distance on the left side is the norm of the error in the image assuming that the output of the camera model evaluated at $\mathbf{p_{opt}}$ gives the distortion-free ML-estimate of the X-centers in the image. Here, the earlier-discussed $\mathbf{\Sigma_i'}$ uncertainty is required. The Mahalanobis distance of two vectors is defined as:

$$d_{Mah,C}^2(a, b) := \left\| a - b \right\|_C^2 = (a-b)^T C^{-1} (a-b). \quad (12)$$

Therefore, this is a well-known form of a special weighted least-squares problem where we weight the measurements with the inverse of their uncertainty. This is the case with the spatial term, as well. There, we use the covariance $\mathbf{\Sigma_i}$ of the 3D location measurements for weighting. The covariance matrices convert the metrical quantities and the pixel quantities into a common, additive dimension on the one hand and put strength on the more certain measurements in affecting the parameters to estimate, on the other hand. However, the ML-estimate $\mathbf{q_i}$ of the spatial features (X-marker centers) is unknown.

Two solutions exist for this problem: either we consider $\mathbf{q_i}$ as parameters (similarily to structure reconstruction applications in machine vision) or we use an approximation of the cost function (11). The first yields that the parameter vector increases significantly, potentially leading to numerical problems at the optimization, the second leads to another (non-ML) cost function that embodies the bidirectional transfer error. This means that when computing the error in the image, we consider the spatial features exact, and when calculating the right-side term we consider the detected image features exact. Thus, $\mathbf{q_i}$ will be the closest point to the spatial feature $\mathbf{x_i}$ that projects exactly into the image feature $\mathbf{x_i'}$. To find $\mathbf{q_i(p_j)}$ at each iteration step j, the "inverse" mapping of φ has to be used that maps an image point into a spatial line and the closest point to $\mathbf{x_i}$ has to be found on this line.

Homography estimation can be used to compute an initial guess for the parameters from the known $\mathbf{x_i}$ and $\mathbf{x_i'}$ feature points because the marker arrangement is approximately planar. From the estimated homography, the rotation matrix and the translation vector can be easily determined. If the arrangement is not planar, then the Direct Linear Transformation (DLT) can be used to find the initial guess. Naturally, this initializing linear step neglects the non-linear radial distortion effect.

V. SIMULATION RESULTS

We will show in the simulations that it is the range of the spatial errors that makes necessary the usage of the novel approach. Using a simple example with the model of a real camera we will show that even small inaccuracies in the marker arrangement cause significant deviations in the image of the markers that competes with the usual practical residual errors resulted by minimizing only geometrical errors.

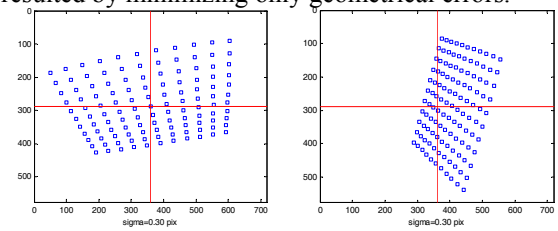

Fig. 4. Synthetic checkerboard images were used to evaluate the effect of feature detection errors on the parameter uncertainties.

A simulated 720x576 camera has been used for this purpose, but the camera has been re-calibrated based on 9 synthetic checkerboard patterns with a corner feature location deviation of 0.30 pixels. This resulted a real-like situation because the covariance of the camera parameters could be determined as well. The camera parameters and uncertainties resulted:
rel.focal lengths: [1159.338 1258.254] ± [2.694 3.085] pixels, skew: 1.045 ± 1.468; principal point: [361.050 287.236] ± [7.046 6.463] pixels; distortion center: [362.668 307.793] ± [4.609 4.363] pixels; radial distortion coefficients: [-0.848 0.118] ± [0.030 0.341]. The estimated standard deviation was 0.29 pixels. 24 synthetic markers and position measurement data has been generated then by considering all the uncertainties in the spatial measurements such as measurement uncertainty in the reference point locations, distance measurements, marker placements. A Gaussian noise with [10,10,2]° pitch-yaw-roll deviations has been added to the marker plates. Uncertainty has been introduced in the aiming process and to the aiming error extraction, as well. Even with the small inaccuracies taken into consideration (from 5 mm in the laser-based distance measurements to 1-2 cm inaccuracy computed for the reference point locations), the uncertainty in the estimated marker locations reached 20-26 cm (at a distance of 40 meters from the reference points.

The exact marker centers have been projected into the image of the camera using the exact camera model, and a detection noise has been added. This modeled the error of the X-detector. The implemented X-detector was evaluated on synthetic images with 5x5 X-pattern tiles with sizes ranging from 10x10 to 45x45 pixels in 5 pixel steps. The tiles were randomly rotated with an angle deviation of 3°. This modeled the skew in the placement of the markers. The exact locations of the X-tile centers were known and therefore the accuracy of the X-detector could be evaluated by performing a high

number of trials. This feature detection was repeated 10 times resulting a total number of detected synthetic X-markers of 250 for each marker size. Interestingly, we found that the X-detector was not sensitive to the size of the X-tiles because this feature detection test resulted a standard deviation ranging from 0.18 to 0.20 pixels independently of the marker sizes. Therefore, we used a deviation of 0.19 pixels in the error modeling of our robust feature detection.

Fig. 5. Synthetic X-marker tiles were used to evaluate the accuracy of the feature-detector. The tiles were randomly rotated with a small amount in order to simulate marker placement skewness, as well.

In order to compare the spatial measurement errors to the error of the X-detection given in pixels, the 99% covariance ellipsoid of each marker measurement was projected in the image of the camera by using the Jacobian of the world-to-image mapping. The size of these ellipsoids increased in function of the depth of the X-markers as shown in fig. 4.

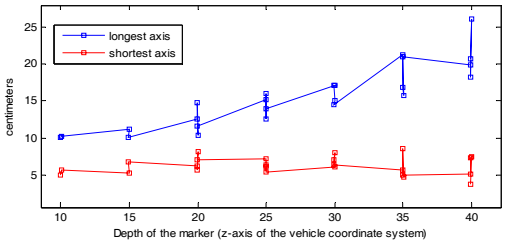

Fig. 6. Axis lengths of the 99% covariance ellipsoids of the spatial measurements in function of the depth (at each depth there were 2 or 4 simulated markers).

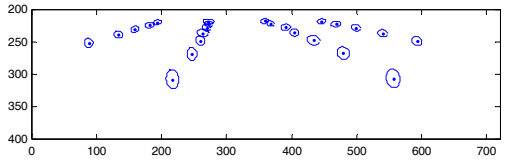

Fig. 7. The 99% covariance ellipsoid of each spatial marker measurement projected in the image of the camera for comparison with the noise of the X-detector.

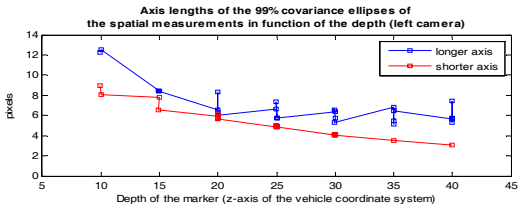

Fig. 8. Axis lengths of the 99% projected covariance ellipsoids of the spatial measurements in function of the depth.

The figures above show that the level of the measurement inaccuracies in the marker location estimation is much higher than the error of a feature detector of sub-pixel accuracy. In the meantime, the error of the marker locations, themselves vary in a relatively wide range. Therefore, it is well suggested to use the weighting matrices discussed earlier in the cost function to make difference between accurately estimated marker coordinates, inaccurate marker location estimations and the relatively accurate feature detection in the image. This shows that it is relevant to introduce co-minimization in 3D space and in the image in far-range calibration.

It is also noticeable that even if the locations of the farther markers are less accurately determined, these errors do not affect the image as much as the nearer markers do. This is clearly due to the perspective effect.

VI. CONCLUSIONS

A far-range camera calibration method has been presented that is applicable for stereo lane detection systems. A method of far-range marker localization has been proposed with two point-measurements by using high-precision laser-based distance meters. For determining the extrinsic camera parameters we proposed a novel optimization method. We minimize geometric errors in the 3D metrical space and in the images simultaneously. This optimization method considers the most information we can have about the noise structure of the measurements. The suggested extrinsic camera calibration method has been paired with the popular one for intrinsic parameter calibration.

The proposed co-minimization method is expected to be more accurate than those that simply minimize geometric error in the image plane when 3D marker coordinates are known with considerable inaccuracy.

The method can be easily adapted to other far-range applications of either stereo or mono vision sensor configurations that require high accuracy.

ACKNOWLEDGEMENTS

This work was supported by the Hungarian National Office for Research and Technology through the project "Advanced Vehicles and Vehicle Control Knowledge Center" (OMFB-01418/2004) which is gratefully acknowledged.

References

[1] Nedevschi, S., et al., "3D Lane Detection System Based on Stereovision" in *IEEE Intelligent Transportation Systems Conference*, Washington D.C., USA, October 3-6., 2004

[2] Trucco, E., Verri, A., *Introductory Techniques for 3-D Computer Vision*, Prentice Hall, New Jersey, 1998

[3] Hartley, R., Zissermann, A., *Multiple View Geometry in Computer Vision*, Second Edition, Cambridge University Press, March 2004

[4] Marita, T., Oniga, F., Nedevschi, S., Graf, T., Schmidt, R., "Camera Calibration Method for Far Range Stereovision Sensors Used in Vehicles" , *Intelligent Vehicles Symposium*, pp. 356-363, Tokyo, Japan, 13-15 June 2006

[5] Zhang, Z., *A flexible new technique for camera calibration*, Technical Report, Microsoft Research, Microsoft Corporation, Redmond, USA, Aug. 10, 2002

[6] Bouguet, J.-I., Caltech Camera Calibration Toolbox for Matlab, 18 October 2006, URL: http://www.vision.caltech.edu/bouguetj/calib_doc/